966
A3 Transmission and Distribution Equipment
PS2 - Decarbonisation of T&D Equipment
Session 2022

Experience in the development of a 170kV/50kA/60Hz HVCB using a CO_2+C_4F_7N mixture

Jeong Cheol KIM, Hyung Choon KIM, Zeljko TANASIC,
Xiangyang YE*, Javier MANTILLA*
Hyundai Electric
Switzerland
xiangyang.ye@hyundai-electric.ch
javier.mantilla@hyundai-electric.ch

SUMMARY

The next generation of environmentally friendly switchgear will not use SF_6. Currently, at the main world manufacturers, products using alternatives based on CO_2 as background gas are under development. The use of FluoroNitriles, 3M Novec™ 4710, C_4F_7N, is addressed by different producers under different trademark names. In most cases, Oxygen is added for health and/or functional reasons. Joining efforts, Hyundai Electric has completed the development of a high-voltage circuit breaker (HVCB) for the rating of 170 kV, 50 kA, 60 Hz using 95% CO_2 + 5% C_4F_7N. The HVCB, part of a Gas Insulated Switchgear (GIS) bay of the same voltage rating, is a three-pole operated in one tank encapsulated design that has fulfilled all the IEC 62271-100 tests. Its performance equals that of its SF_6 counterpart, at an identical equipment size yet a reduction of the Global Warming Potential (GWP) of the gas mixture of more than 98%.

Using modern one-dimensional simulation (1D) and Computational Fluid Dynamics (CFD) off-shelf tools complemented with in-house developed models and material data, the design and successful development of a high voltage circuit breaker using an environmentally gas mixture using only C_4F_7N and CO_2 was completed. Multi-Objective Optimization (MOO) coupled with a 1D system model, allowed us to reach a deep understanding and correlation of the main variables that determined interruption during the thermal and dielectric regimes. The MOO approach cemented the basis for the development of a machine learning (ML) methodology applied in the Design of Experiments (DOE), simulations, and design of high voltage equipment. The results of the simulations were validated in certified laboratory tests with prototypes and the final product.

Short-line fault 90% and Terminal fault with 100% of the short circuit current presented challenges to overcome. The dependency of the thermal clearing capability with the gas temperature, the changed gas properties, associated flow fields, and the dielectric soundness of the gas mixture in the exhaust volumes during the recovery voltage phase were issues that could only be solved through simulation and testing.

The absence of Oxygen presented challenges in terms of byproducts management. The approach taken to solve and manage the solid Carbon (C) also known as soot, estimations on the toxicity of the generated CO, and considerations around it are presented. The absence of O_2 also presented opportunities in terms of improved temperature fields, slightly increased dielectric strength, lower evolutional GWP, and extended gas lifetime. Furthermore, other important operational aspects that the absence of O_2 poses are also discussed such as the reduced oxidation of metallic parts and complete elimination of risks in gas handling and runaway exothermal reactions coupled with O_2.
This work summarizes the experience of designing the first CB of its kind in rating and gas mixture, the required simulations, and the experimental results. It presents considerations on the future of this technology and its role and scalability in carbon-neutral electrical networks.

KEYWORDS

FluoroNitriles (C_4F_7N), High Voltage Circuit Breaker (HVCB), Global Warming Potential (GWP), Multi-Objective Optimization (MOO), Computational Fluid Dynamics (CFD), Toxicity, Soot, Gas lifetime, Carbon-neutral, Current Zero (CZ), Polytetrafluoroethylene (PTFE), Transient Recovery Voltage (TRV)

1. INTRODUCTION

The use of Fluorinated molecules from the 3M Novec™ family has become the standard in the efforts to replace SF_6 in the electrical industry for MV and HV applications. The vast majority of utilities worldwide are undertaking efforts to decarbonize their switchgear fleet following different time horizons as decided at country level during the 26th United Nations Climate Change conference of 2021. To cover the current and future demand for SF_6-free switchgear, Hyundai Electric has started the decarbonization and modernization of its HV switchgear portfolio. In this work, the experience of developing a first-of-its-kind SF_6-free HVCB is presented.

2. BOUNDARY CONDITIONS

2.1 Ratings

In table I the ratings reached in the development project are presented.

Rated voltage	Un	kV	170
Rated frequency	f	Hz	50/60
Rated normal current	In	A	4000
Rated short-circuit current	Isc	kA	50
Time constant	τ	ms	45
Rated operating sequence	Oseq	-	O-0.3s-CO-3min-CO
Indoor/Outdoor	-	-	Both
Operating mechanism	OM	-	Hydraulic
Operation	-	-	TPO
Mechanical endurance	M	-	M2
Electrical endurance	EE	-	E1
Capacitive switching class	CC	-	C2
Temperature range	Tmin-Tmax	°C	-25 to +40
Cycles	Cy	-	3
First-pole-to-clear factor TF	kpp	-	1.3
First-pole-to-clear factor OoP	kop	-	2.0
Capacitive voltage factor	kc	-	1.4

Table I. Developed ratings

2.2 The O_2-free Gas Mixture

In table II, the used gas mixture and related pressures are presented.

Carbon dioxide percentage	CO_2	%	95.3%
FluoroNitriles percentage	C_4F_7N	%	4.7%
Rated gas mixture pressure for interruption @20°C	Pfill CB	bar_abs	9
Rated gas mixture pressure for insulation @20°C	Pfill compartments	bar_abs	8

Table II. Gas mixture

The decision to pursue an O_2-free gas mixture was taken based on operational, technical, and intellectual property matters. Advantages and disadvantages were analyzed and ultimately the absence of O_2 presented opportunities and advantages before unexplored. These are summarized in Table IV.

2.3 Thermodynamic Considerations

Understanding the thermodynamic behavior of the gas mixtures and involved species is fundamental to grasping the evolution of the different gas components, from a new condition, through different switching events, up to decommissioning of the equipment. Not only the steady-state nature of the components, i.e. before and after a switching event, but also the transient behavior (i.e. during switching), the generation of temporary radicals, and the impact that these molecules have on the quenching and/or dielectrics mechanisms, unveils possible ways to overcome performance limitations that otherwise are not visible when a simple single-component approach is taken. Knowing what molecules and other species exist at any point in time is key for the design.

The study of the species generated during thermal decomposition proved useful during the development both for functional (dielectrics, arc quenching) and operational (toxicity, material compatibility) issues. Using the open-source software Cantera [1] under a Python scripting environment and the NASA input file described in [2] in chemical equilibrium with the C_4F_7N, the thermodynamic behavior and chemical reactions of the gas mixture under different conditions were studied. The main focus was the thermal decomposition of the mixture along with a typical switching operation, the radicals form at the different stages, the final byproducts, and the associated change in GWP of the resulting mixture.

Mixtures of CO_2 (95% or 85%), C_4F_7N (5%), and O_2 (10%) were studied using the average temperature in the arcing zone of the interrupter at the rated gas mixture pressure for interruption. During arcing, PTFE is ablated due to the radiative heat transfer with a vapor temperature of about 3500K. The ablation causes the pressure to increase in the arcing zone and all connecting volumes. PTFE vapor (C_2F_4) is unstable and undergoes further decomposition into 69% F, 28% C_2F_2, and small parts of C2 and C3. After current zero and associated temperature reduction, C_2F_4 does not recombine forming instead more stable compounds. The typical PTFE ablation mass is around ~10 g per switching operation, i.e., the mole fraction of PTFE vapor can reach about ~10% in an arcing zone with a volume of ~4 Litre. This mole fraction of PTFE is added to the gas mixtures evaluated to consider its contribution to the chemical reactions during the arcing process.

The simulation input data and results are presented in figures 1 to 3.

In figure 1, the temperature of the arcing zone, calculated in a CFD environment is correlated to the current for a 16.6 ms, SLF90, 50 kA arcing time.

In figures 2 and 3, the thermal decomposition processes of the evaluated gas mixtures with 10% PTFE are shown. During arcing all species are decomposed into atoms, electrons, and ions. After CZ, the gas cools down to temperatures below their dissociation limits, and the species are recombined either into their original molecules or into other stable molecules.

In figure 2, the thermal decomposition of the CO_2 and C_4F_7N plus PTFE is presented. At each stage during high current, and/or CZ different species are formed, relevant to the understanding and the design of the interrupter. The final resulting species, in this case, are CO_2, CO, CF_4, and N_2. A negligible percentage of COF2 is remaining in the calculation. Due to its instability, this molecule decomposes further finally forming CO_2 and CF_4.

In figure 3, a similar process occurs, yet in the presence of O_2, in the final byproducts CO and COF2, both are completely avoided.

In reality, CO has been measured in mixtures containing O_2 [3], which suggests that either a much higher percentage of O_2 is needed, -which might be impractical, or that is completely unavoidable.

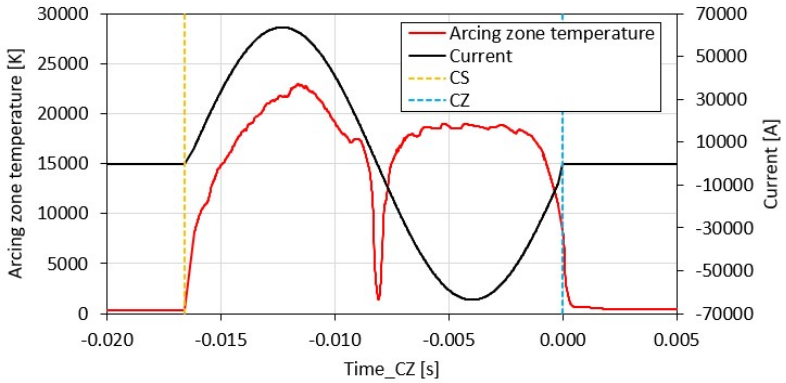

Figure 1. Average temperature in the arcing zone for a SLF90, 50kA, 60Hz interruption, correlated to the current used for the species analysis with Cantera

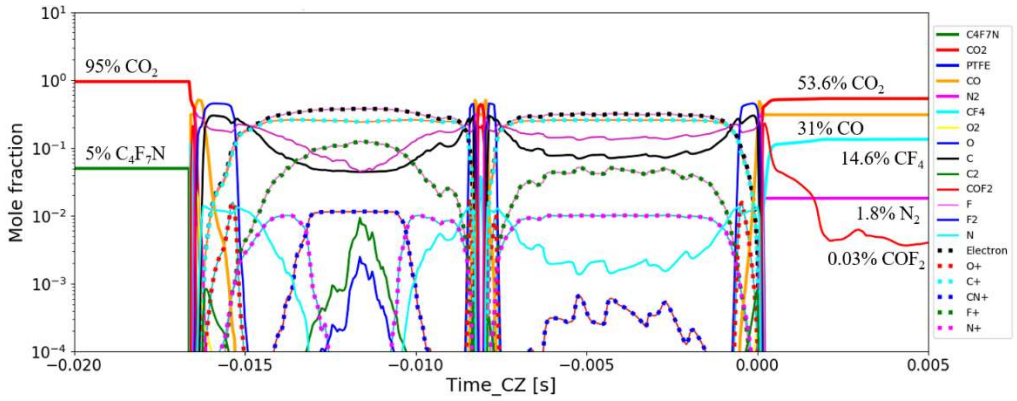

Figure 2. Thermal decomposition of 95% CO_2 and 5% C_4F_7N gas mixture with 10% added PTFE

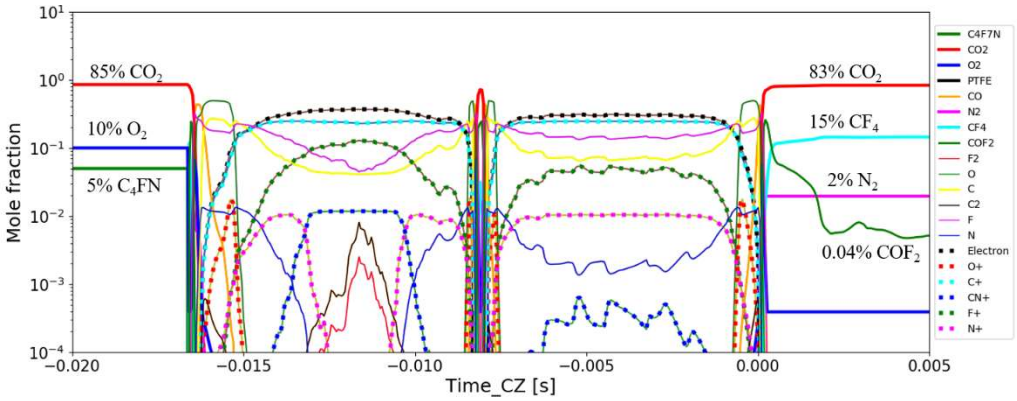

Figure 3. Thermal decomposition of 85% CO_2, 5% C_4F_7N, and 10% O_2 gas mixture with 10% added PTFE

Two main takeaways from the thermodynamic analysis presented in figure 2 and 3, using the boundary conditions of figure 1, are:

- From an operational viewpoint, both cases (with and without O_2) produce similar byproducts, none of which affects the functioning of the equipment.
- From a toxicity viewpoint, the mixture with O_2 produces less amount of toxic byproducts. Yet, in both cases, the same category of Personal Protective Equipment (PPE) is needed.

It needs to be noted that the analysis considers the full consumption of the C_4F_7N molecule. In reality, whereas this is true in specific locations, in the overall volume, a new steady-state including undecomposed C_4F_7N is reached after the switching event.

3. TESTING

Simple calculations, 1D to 3D, FEM, CFD simulations, and modular testing, all of these instruments were highly used in the early stages of the project but also accompanied the development during the testing phase. In table III a summary, categorized by type of test duty, the expected challenges, the surfaced challenges, and the results is presented.

Test Duty	Possible issue	Real issue faced	Result
Mechanical Endurance – M2	Due to the lower density characteristic of the mixture, sooner structural wear and/or issues during the final voltage condition check.	None	Passed
Capacitive Switching – C2	Issues with pre-conditioning and associated gas mixture decomposition.	None	Passed
T10, T30, OP	Weaker early dielectric recovery during the first microseconds.	None	Passed
T60	None	None	Passed
SLF75	Higher and longer-lasting 1st line peak vs. PAC	None	Passed
SLF90	Highest possible thermal interruption stress	Incorrect/insufficient flow conditions in the arcing zone. Solved after simulation-assisted test iterations.	Passed
T100s	Mixture homogeneity during O-CO and possible associated issues for clearing. Mixture homogeneity and weak spots in the exhaust region.	O-CO no issue. Exhaust voltage breakdowns during early designs. Solved after design modifications.	Passed
T100a	Highest temperature/pressure input might cause dielectric and/or structural issues.	None	Passed
E1	Gas mixture dielectric capability along with the procedure.	None	Passed
Temperature Rise	Lower heat transfer properties of the gas mixture might cause hotspots	None	Passed

Table III. Summary of test results, expected and real challenges solved

The table above does not mean that an existing SF_6 CB was retrofitted with an alternative gas mixture and issues only in SLF90 and T100s appeared. The starting point of the testing campaign was on an already modified interrupter to be used with a CO_2 + C_4F_7N mixture using simulation results.

3.1 Short Line Fault

As described in Table III, SLF90, presented some challenges to overcome during the development process. Fundamentally the issue was an inappropriate allocation of the main variables responsible for thermal interruption along the stroke of the interrupter.

3.1.1 1D System Modelling and MOO

A 1D system model in Amesim [4] was used to simulate the behavior of the HVCB during opening operations. The model represents the gas volume with corresponding surfaces, orifices, and valves. The OM is not modeled instead, the movement is given as input from measurements. The ablation behavior of the PTFE nozzles uses the two-zone model as described in [5]. A no-load simulation was used as a first-level validation of the geometrical representation to the real HVCB measured pressure in the compression volume. Calibration in terms of load operations required finding the ablation coefficient to match the measured pressure in compression volume. In literature, this value is given as 17 mg/kJ [5] but can vary from 12 mg/kJ to 35 mg/kJ depending on nozzle material and injected current.

In the past, a lot of work was put to explore what objectives influence the clearing capability process. Different techniques were applied to better classify clearing and failing during the early development phase [6]. Often the pressures in the compression or heating volumes were taken as a key parameter mostly due to the relatively easiness to measure. However, within a simulation model, all quantities can be used for evaluation. In that sense, two objectives were defined as proxies of interruption: objective 1 (*obj1*) Eq.(1), as the pressure in the arc zone volume at current zero, and objective 2 (*obj2*) Eq.(2) as the integrated temperature in the arc zone volume during the last half-wave of the short circuit current.

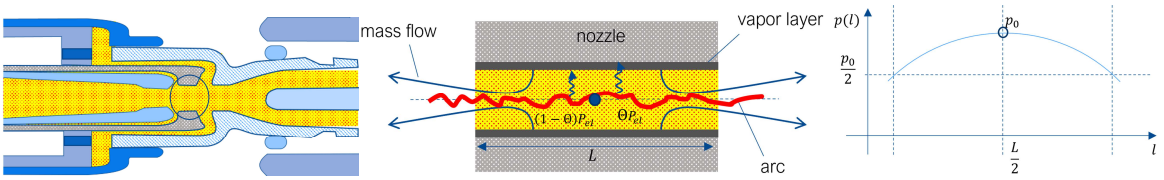

Figure 4. Arc zone cross-section, 2-zone model, and, prescribed pressure distribution

The objectives are summarised below, whereas *obj1* is to be maximized and *obj2* minimized.

$$obj_1 = P_{CV@CZ} \quad (1) \qquad obj_2 = \overline{T}_{arcZone} = \frac{1}{t_2 - t_1}\int_{t_1}^{t_2} T_{arcZone}\,dt \qquad \begin{matrix} t_1 = t_{CZ} - \frac{T}{2} \\ t_2 = t_{CZ} \end{matrix} \quad (2)$$

Where $P_{CV@CZ}$ is the pressure in the compression volume at current zero and $T_{arcZone}$ is the temperature in the arc zone volume averaged over the arcing time from contact separation (t_1) until extinction (t_2).
It is to be noted that the variable's space needs to be kept on a manageable value considering that the number of simulations and thus calculation time, increases quadratically with these. The trade-off between CPU time, convergence speed, and accuracy need to be taken into account.
Multi-Objective Optimisation (MOO) refers to the optimization of several objectives inside a predefined variable space simultaneously. The problem becomes challenging when the objectives are of conflicting characteristics to each other as *obj1* and *obj2* are. Solving such problems, with or without the presence of constraints, a set of trade-off optimal solutions are produced, known as the Pareto-optimal solution. Given the multiplicity of solutions, these problems were solved suitably using evolutionary algorithms (EA), a population-based approach in which more than one solution participates in the solution-finding process. It evolves and a new population of solutions in each iteration is created. The evolutionary process resorts to processes of initialization, crossover, mutation, and elitism as described in [6]. Together with the algorithm described in [7], optimal design explorations through MOOs were carried out using Amesim coupled with Python, reproducing several tested designs resulting in a map of performance zones differentiated by the clearing likelihood (Figure 5).
Figure 5, shows the Pareto front of one of the several MOOs performed along with the project. The x-axis represents the pressure in the compression volume at current zero (P at CZ). This variable is directly correlated with the clearing capability of the interrupter. The y-axis represents the integral of the Temperature in the arcing zone (int (T)), which is inversely correlated to clearing capability. The blue dots represent reproduced successful interruptions of the same HVCB but with slightly changed geometrical properties (e.g., auxiliary and main nozzle length) at different arcing times. Knowing the results of the different tests, the plot is divided into zones where red indicates a zone where the interrupter failed, and blue a zone where the interrupter cleared the fault. A transitional zone where both regions meet and the outcome is uncertain is also shown.

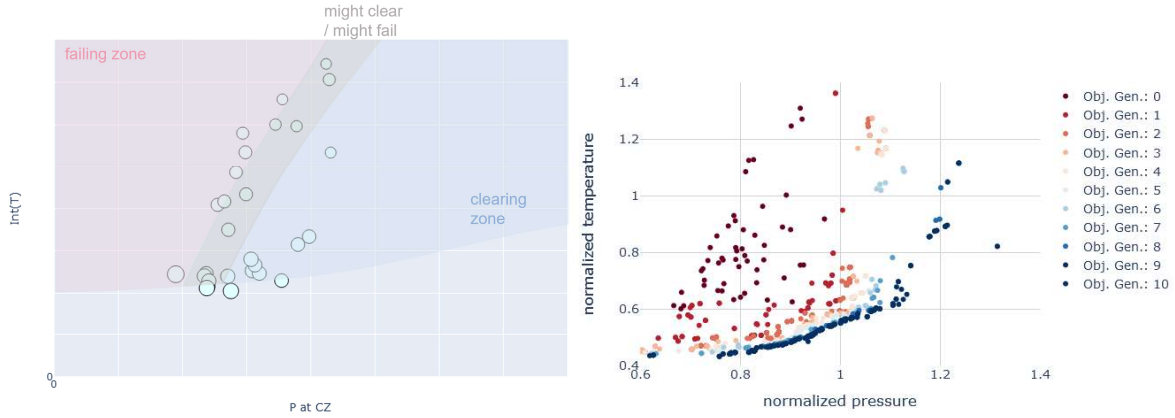

Figure 5. Zones of failure and success derived from successful tests indicated with circles (left) and applied MOO and resulting Pareto frontier to a HVCB model (right)

On the right, the outcome of a MOO run is visualized where the fitness of the initial population is shown in dark red and the final generation 10 represents the resulting Pareto front in dark blue. This specific analysis helped to uncover the influence of specific design changes that ultimately led to the selection of several designs variants one that finally fully cleared SLF90 with margin.

3.1.2 CFD Prediction and Validation

Once a set of promising variants was identified and the relationship between several physical and circuit variables determined, the final step before testing was through CFD study of the behavior of the interrupter while clearing including much more complete and closer to reality physical fields that 1D simulations are not meant to capture. In figure 6, a selected cleared shot is shown with a pressure build-up comparison between measurement and simulation. An error band on the simulated pressure is added to visualize the unavoidable error arising from the tool, the models, and the boundary conditions. It is however clear that measurement and simulation are in very close agreement with each other.

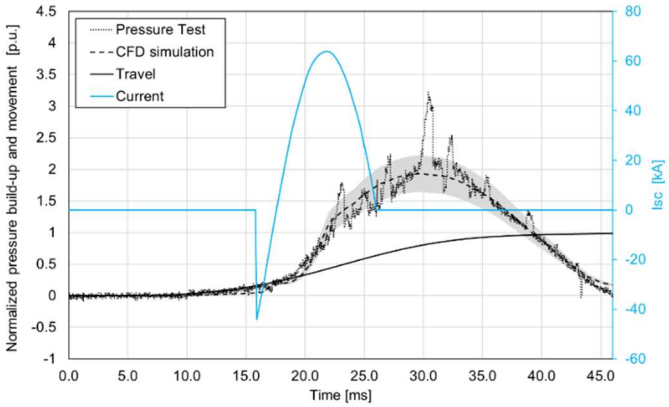

Figure 6. Selected SLF90 pressure build-up comparison between measurement and simulation.

The excellent agreement between simulation and measurements can be attributed to a great extent to:

i. The correct modeling of the 3D geometry to a proper 2D equivalent. A good part of the geometry is axisymmetric, yet key components like the tulip (female arcing contact), exhaust tube, etc. are not. The correct modeling of these is key.
ii. Accurate modeling of the thermodynamics and decomposition reactions along with a switching operation. Being able to reflect the correct species and their impact in the different fields (e.g. pressure, temperature, etc) allows for a closer depiction of reality.
iii. The inclusion of heat transfer also into the solid bodies of key regions in the interrupter.

3.1.3 The PAC vs 1st Line Peak Race

Thermal interruption in a HVCB is decided in the few microseconds before and after current zero. The amplitude and duration of the Post Arc Current (PAC) is a relative indicator of the cooling of the arcing zone and the behavior of the residual current flowing between the arcing contacts. Combined with the early characteristic of the line side TRV in SLF test duties, characterized by an increase of the voltage drop between the CB terminals, determines whether the CB interrupts the fault, or if on the contrary the increase of the electrical field and the drifting electrons is stronger than the cooling of the region and a reignition occurs.

In figure 7, the frequency and cumulative probabilistic distribution of the times to PAC peak after CZ of selected cleared SLF90 tests is shown. For the rating of the developed switchgear in this work, the time to the TRV 1st line peak is ~2.5 µs for SLF90 and ~6.4 µs for SLF75. It is noted that the majority of the decision times are distributed around 3 µs, signalizing sufficient clearing power beyond the 1st line peak inflection. It is possible, that some combinations of the CB flow conditions and fault parameters can produce conditions harder for clearing. It is worthy and necessary always to closely observe the behavior of SF_6-alternatives in this timeframe.

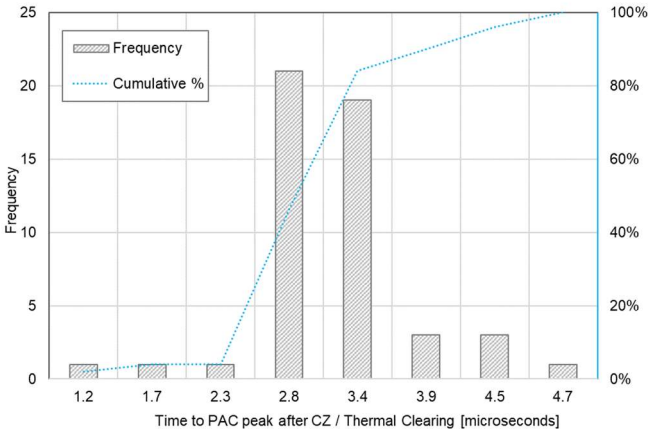

Figure 7. Frequency and cumulative distribution of the time to post-arc current peak after CZ of several SLF90 cleared shots along with the development

Ultimately the combination of 1D simulation, MOO, fine-tuning with CFD and close observation of the phenomena around CZ led to the final design that withstood with margin both SLF test duties.

3.2 Symmetrical Terminal Fault 100%

T100s presented a second challenge to overcome during development. Fundamentally the issue was a weakness in the exhaust system where late breakdowns in the range of milliseconds occurred during the Recovery Voltage (RV) phase. It was unclear if the dielectric issues were caused by a weaker gas region (low density), soot, surface roughness-related matters, or a combination of all.

The only meaningful way to approach the issue was with 2D and 3D CFD simulations where besides the arc model, the multi-component gas mixture and decomposition equations as explained in [8] of CO_2 and C_4F_7N were used. Also included in the simulation, were the solid parts (metals and polymers) of the interrupter to account for the respective heat transfer mainly through convection into these. The capacitive electrical field was simulated after CZ using the multi-physics solver of the tool.

In figure 8, a 2D CFD simulation of the completed interrupter is shown with color-coded plots of the distribution of the total gas mixture temperature (a) top) and mass fraction of C_4F_7N (b) bottom) and the ratio of the local electrical field to the local density (E/ρ) (b) top), correlated to the local breakdown voltage (b) bottom).

In this simulation already corrective measures had been taken and the main variables checked.

In a), it can be seen that the mass fraction of C_4F_7N in the arcing zone is at a minimum due to the local decomposition caused by the arc plasma and temperature fields above the dissociation temperature of C_4F_7N whereas in the exhaust towards the tank virtually no decomposition takes place.

In b), the E/ρ value and associated local breakdown voltage are presented. Tendentially it can be said that the plug side has a lower withstand limit due to the less efficient exhaust system on that side, yet it is more than enough to hold the TRV and RV voltage after the current has been interrupted.

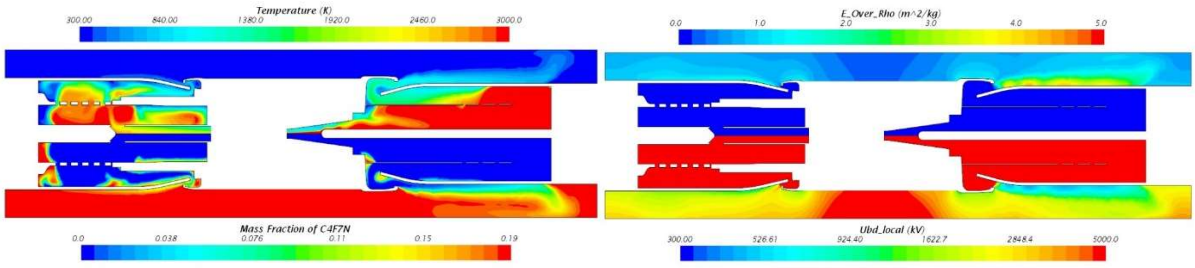

a) b)

Figure 8. Colour coded CFD plots of the main analyzed variables and ratios at T100s

The breakdown voltage is calculated through scripting in the tool using Eq. (3), where *Ecr* is the breakdown electric field strength of the gas mixture at 1 bar, *ρ0* the density at 1 bar, and 300 K, (E/ρ)max

the maximum value of E/ρ calculated at 1 V, *f(T)* a predefined temperature function considering the dielectric behavior beyond the dissociation limit and k_R the roughness factor. *f(T)* and k_R of empirical nature are calibrated based on the test results.
In figure 9 the evaluated breakdown voltage of the T100s O-CO operation after CZ of the first opening (CZ1) and second opening (CZ2) are shown. It is compared with the TRV, and RV envelope as prescribed by the standard to verify whether its value is high enough in the early recovery phase after CZ (microseconds) but also during the late recovery phase at milliseconds. In both cases, despite a decrease in withstand for the second O-operation, the value is high enough to cope with requirements. This signalizes the positive effects of the modified design in the exhaust where the gas was cooled down through different mixing mechanisms and redirection of the gas towards less dielectric sensitive regions. Ultimately it was determined that the issue was solely due to a weaker combination of gas quality (density) in higher electric field regions. The other two suspected reasons, soot, and surface roughness were discarded. The problem was solved in one iteration and the test passed.

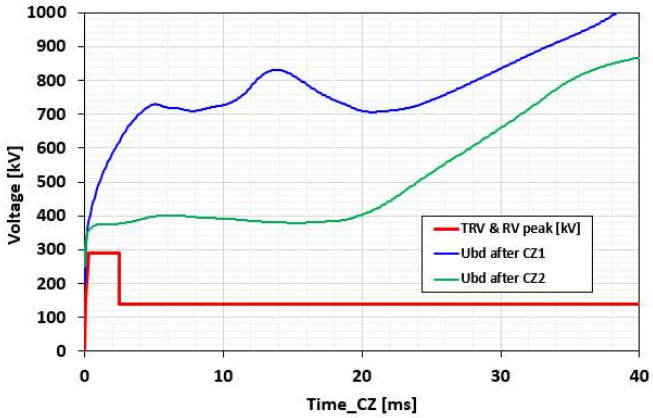

Figure 9. Calculated *Ubd* at T100s O-CO conditions

$$U_{bd} = \frac{Ecr/\rho_0}{(E/\rho)_{max}} * f(T) * k_R \qquad (3)$$

4. CONCLUSIONS AND OUTLOOK

The sophistication of modern software tools has considerably increased in the last years. Today Multi-species/physics/bodies simulation allows a much closer approach to very complex problems. Yet, there is no single tool in the market that will off-the-shelf support the design and development of non-SF_6 HVCB. Physics models, gathered during decades of experience need to be coded, refined and validated constantly to produce useful results. The existing commercially available software packages need to be extended with in-house models coded in different languages, maintained with software upgrades, and benchmarked with available experimental data.
In this work, the results of the use of applied experience in simulation, design, and development of eco-friendly HVCB are presented. The developed product is the first of its kind in rating and simplicity of the gas mixture. It opens the door for a new generation of high voltage switchgear where a minimum carbon footprint is part of the design on top of robustness and quality. The avoidance of O_2 presented challenges but also opportunities to explore. The main findings are summarized in Table IV. In the long run, both solutions present advantages and disadvantages worth considering. The final choice rest on the user side.

Aspect	With O_2	Without O_2	Comment
Toxicity	++	+++	CO capture is less. Yet the existing SF_6 PPE and HSE measures are enough.
Soot Generation	++	+++	More soot is theoretically generated. Yet there was no experimental evidence of this or that the amount generated represented a problem.
Oxidation of metal parts	+++	-	In the absence of O2, oxidation of metals is not an issue.

Gas handling	More complicated	Easier	One gas bottle less to manage represents an immense advantage in gas handling.
Runaway combustion	Possible	Not possible	Mistakes during O_2 filling might open the possibility of runaway combustion associated with O_2. Several materials used in HVCB can burn, and a spark is given.
Gas lifetime	Shorter	Longer	Having O_2 in the mixture will produce hotter temperature fields during interruption leading to an increase in the decomposition of the C_4F_7N.
Electrical lifetime	Shorter	Longer	The presence of O_2 increases nozzle ablation, thus reducing the lifetime of one of the four variables as explained in [9]
Evolving GWP of the mixture	Low	Lower	With increased nozzle ablation caused by O_2, there is an increment in CF_4 production which has a GWP of 6500 [10]. This marginally increases the GWP of the mixture after switching [11].

Table IV. Learnings of the Avoidance of O_2 in the Gas Mixture

In figure 10, the installed GIS in the Wang-gok substation in Korea is shown. It has been in operation since early 2021. Several projects are undergoing to modernize the Hyundai Electric HVCB portfolio in the direction of environmentally friendly and smart switchgear. That this technology is easily scalable, ratings up to 420 kV are in the near time horizon.

Figure 10. Complete GIS in operation in the Wanggok substation in South Korea

Table I and Table II, address the main GIS specifications of the equipment shown in figure 10 with regards to ratings and gas mixture. The size of the bay is the same as the existing SF_6 product. 99% reduction of greenhouse gas emissions was achieved in this project. The current transformer, bus disconnectors, and earthing switch all were transferred from the SF_6 product with some minor modifications on the disconnector. The product is qualified for ISO 9001 (Quality), ISO 14001 (Environmental management), and ISO 18001 (Occupational health and safety management).

BIBLIOGRAPHY

[1] "Cantera." https://cantera.org/ (accessed Jan. 14, 2020).

[2] B. J. McBride, *Coefficients for calculating thermodynamic and transport properties of individual species*. [Washington, DC] : National Aeronautics and Space Administration, Office of Management, Scientific and Technical Information Program ; 1993.
[3] J. D. Mantilla, Claessens, and Kriegel, "Environmentally friendly perfluoroketones-based mixture as switching medium in high voltage circuit breakers," *e-cigré*, 2016. https://e-cigre.org/publication/A3-113_2016 (accessed Jun. 03, 2019).
[4] "Simcenter Amesim | Siemens Software." https://www.plm.automation.siemens.com/global/en/products/simcenter/simcenter-amesim.html (accessed Nov. 30, 2021).
[5] "Simulation von Gasströmungen in SF_6-Selbstblasschaltern bei Kurzschlussabschaltung by Claessens, Max," *RWTH Aachen: Shaker Verlag 1997*.
[6] S. Ivanov and A. Ray, "Application of multi-objective optimization in the design and operation of industrial catalytic reactors and processes," *Physical Sciences Reviews*, vol. 1, Jan. 2015, DOI: 10.1515/psr-2015-0017.
[7] K. Deb, A. Pratap, S. Agarwal, and T. Meyarivan, "A fast and elitist multiobjective genetic algorithm: NSGA-II," *IEEE Transactions on Evolutionary Computation*, vol. 6, no. 2, pp. 182–197, Apr. 2002, doi: 10.1109/4235.996017.
[8] S. Brynda, Y. Park, H. Sohn, T. H. Song, X. Ye, and J. D. Mantilla, "Theoretical and Practical Behaviour of Eco-friendly SF_6 Alternatives in High Voltage Switchgear," in *e-cigre*, Aug. 2020, pp. a3-119. Accessed: Feb. 09, 2021. [Online]. Available: https://e-cigre.org/publication/SESSION2020_A3-119
[9] N. Gariboldi and J. D. Mantilla, "Electrical wear in high voltage circuit breakers using SF_6-alternatives," *The International Electrical Testing Association Journal*, vol. 43, no. 2, p. 9, Summer 2021.
[10] P. Forster *et al.*, "Changes in Atmospheric Constituents and in Radiative Forcing," p. 106.
[11] X. Ye and J. D. Mantilla, "Global Warming Potential Considerations for Gaseous SF_6 Alternatives Along the Switchgear Lifetime," *CIGRE B&H Electrical Engineering*, p. 7, Sep. 2021.